Giant Unilamellar Vesicles Containing Phosphatidylinositol(4,5)bisphosphate: Characterization and Functionality

Kévin Carvalho,*† Laurence Ramos,† Christian Roy,* and Catherine Picart*

*DIMNP, Dynamique des Interactions Membranaires Normales et Pathologiques, Centre National de la Recherche Scientifique, UMR 5235, Université Montpellier II et I, Montpellier, France; and †Laboratoire des Colloïdes, Verres et Nanomatériaux, Centre National de la Recherche Scientifique, UMR 5587, Université Montpellier II, Montpellier Cedex 5, France

ABSTRACT Biomimetic systems such as giant unilamellar vesicles (GUVs) are increasingly used for studying protein/lipid interactions due to their size (similar to that of cells) and to their ease of observation by light microscopy techniques. Biophysicists have begun to complexify GUVs to investigate lipid/protein interactions. In particular, composite GUVs have been designed that incorporate lipids that play important physiological roles in cellulo, such as phosphoinositides and among those the most abundant one, phosphatidylinositol(4,5)bisphosphate (PIP_2). Fluorescent lipids are often used as tracers to observe GUV membranes by microscopy but they can not bring quantitative information about the insertion of unlabeled lipids. In this study, we carried out ζ-potential measurements to prove the effective incorporation of PIP_2 as well as that of phosphatidylserine in the membrane of GUVs prepared by electroformation and to follow the stability of PIP_2-containing GUVs. Using confocal microscopy, we found that long-chain (C16) fluorescent PIP_2 analogs used as tracers (0.1% of total lipids) show a uniform distribution in the membrane whereas PIP_2 antibodies show PIP_2 clustering. However, the clustering effect, which is emphasized when tertiary antibodies are used in addition to secondary ones to enhance the size of the detection complex, is artifactual. We showed that divalent ions (Ca^{2+} and Mg^{2+}) can induce aggregation of PIP_2 in the membrane depending on their concentration. Finally, the interaction of ezrin with PIP_2-containing GUVs was investigated. Using either labeled ezrin and unlabeled GUVs or both labeled ezrin and GUVs, we showed that clusters of PIP_2 and proteins are formed.

INTRODUCTION

Phosphoinositides are a particular class of lipids present in cell membranes that have very important physiological roles (1). Their structure shares a common inositol ring bearing one, two, or three phosphate groups and their glycerol moieties link both a saturated and an unsaturated alkyl chain. Phosphatidylinositol(4,5)bisphosphate ($PI(4,5)P_2$ or PIP_2) is the most abundant phosphoinositide at the plasma membrane. It has the ability to interact with a wide range of proteins (2–4). It is now well documented that PIP_2 regulates the cytoskeleton/plasma membrane interactions, membrane trafficking, exocytosis, endocytosis, and the activation of enzymes (2,5–7). A great deal of work is dedicated to the understanding of the role of PIP_2 in cellulo, using fluorescent tools (8). In addition, studies in biomimetic systems, including large unilamellar vesicles (LUVs) (9,10), supported lipid bilayers (SLBs) (11,12), and giant unilamellar vesicles (GUVs) (13,14) have emerged during the past years to elucidate the molecular mechanisms of protein/lipid interactions in well defined systems composed of a limited number of constituents. Thus, LUVs allow one to carry out quantitative determination of affinity constants by co-sedimentation assays (15) or fluorescence correlation spectroscopy (16). In addition, SLBs can be observed by atomic force microscope, allowing one to follow in situ protein/membrane interactions (12) or to visualize lipid domain formation (17). Nevertheless, GUVs are more ''cell mimics'' than LUVs and SLBs as their size (from ~5 to ~40 μm) and membrane curvature are similar to those of cells and as they can be observed using a light microscope (18,19). The protocol for producing LUVs seems rather well established (15) and various phosphoinositides have already been incorporated in LUVs (14). Their characterization is possible by means of electrophoretic (i.e., ζ-potential) measurements to check whether PIP_2 is effectively incorporated in the LUVs. ζ-Potential measurements also allow investigations of ion/vesicles (20) or protein/vesicles interactions (21). Recently, electrophoretic measurements also were used for measuring the ζ-potential of LUVs fabricated from a lipid mixture that contains various amounts of phosphoinositides (22).

Very generally, the preparation of GUVs is recognized to be much less straightforward than that of LUVs. Two main methods for preparing GUVs are widely used: the gentle hydration method (23) and electroformation (24). The former, although much simpler, is known to give a poor yield in unilamellar vesicles and a high percent of vesicles presenting defects, but it can be used in physiological media (media of relatively high ionic strength) (25). The latter gives a high yield of unilamellar vesicles but is restricted to low ionic strength media due to the application of an electric field (25). Furthermore, it has also been shown that the presence of a too large fraction of negatively charged lipids does not favor the

Submitted November 30, 2007, and accepted for publication May 1, 2008.

Address reprint requests to Catherine Picart, E-mail: catherine.picart@univ-montp2.fr.

Editor: Enrico Gratton.

0006-3495/08/11/4348/13 $2.00

doi: 10.1529/biophysj.107.126912

formation of unilamellar vesicles with both methods. In addition, the size of the GUVs renders them more fragile and more difficult to manipulate than LUVs. A survey of the literature indicates that studies on GUVs containing phosphoinositides are only emerging (Table 1). The gentle hydration method has been mostly chosen to prepare PIP_2-containing GUVs (26–28) and only three recent studies used electroformation (13,14,29) with unlabeled PIP_2 and a small percent of labeled dipyrromethene boron difluoride (BODIPY) tetramethylrhodamine PIP_2 (TMR-PIP_2) or BODIPY FL PIP_2 (FL-PIP_2). However, PIP_2 is known to be a micelle-forming lipid (29,30) due to its large polar headgroup, and short chains TMR-PIP_2 and FL-PIP_2 are also known to not partition easily into a phosphatidylcholine membrane (29). Thus, it seems important to check, on the one hand, that PIP_2 is effectively incorporated in the membrane of GUVs and, on the other hand, whether fluorescent PIP_2 molecules and PIP_2 antibodies are reliable indicators of the incorporation of native PIP_2 within vesicles.

In this work, our aim was to investigate the conditions for the effective formation of GUVs containing PIP_2 by electroformation to subsequently use these GUVs for investigating protein/membrane interactions. As fluorescent lipids are useful and often needed to carry out confocal microscopy observations, we will also investigate the conditions for incorporation of FL-PIP_2 and TMR-PIP_2 as tracers in GUVs. ζ-Potential measurements on GUVs, direct incorporation of fluorescently labeled PIP_2, and antibody-labeling of GUVs will prove that PIP_2 is effectively and quantitatively incorporated in the membrane of GUVs.

Finally, we will show that ezrin, a protein that is known to interact via its FERM (4.1, ezrin, radixin, moesin) domain with PIP_2 molecules inserted in supported lipid bilayers (12) and with large unilamellar vesicles containing PIP_2 (22), is able to induced PIP_2 reorganization on interaction with the membrane of GUVs.

MATERIALS AND METHODS

Lipids and buffers

1,2-Dioleoly-*sn*,-glycero-3-phosphatidylcholine (DOPC) and 1-palmitoyl-2-oleoyl-*sn*-glycero-3-phosphatidylserine (POPS) were obtained from Avanti Polar Lipids (Alabaster, AL). Cholesterol (Chol) was obtained from Sigma (St. Quentin Fallavier, France). The ammonium salt of L-α-phosphatidylinositol(4,5)-bisphosphate (PIP_2) was purchased from Lipid Products (Surrey, Great Britain). The PIP_2 is extracted from natural source and thus contains both unsaturated and saturated acyl chains. BODIPY-TMR-PI(4,5)P_2, (TMR-PIP_2, reference C-45M16a for the C16 chain and reference C45-M6a for the C6 one), BODIPY-FL-PI(4,5)P_2 (FL-PIP_2, reference C-45F16a for the C16 chain and reference C-45F6a for the C6 one) were purchased from Echelon Bioscience (Tebu-Bio, Le Perray en Yvelines, France). These BODIPY-PIP_2 are fluorescent analogs of PIP_2 and contain only saturated alkyl chains with the dye grafted at one of the alkyl chains (the structures are available at http://www.echelon-inc.com). Monoclonal antibodies (IgG_{2B}) against PIP_2 were bought from Assay Designs (Ann Arbor, MI). Secondary and tertiary antibodies (rabbit anti-mouse coupled to Alexa 568 (RAM-Alexa 568), unlabeled goat anti-mouse antibody (GAM), and donkey anti-goat antibody coupled to Alexa 488 (DAG-Alexa 488) were bought from Molecular Probes (Eugene, OR).

Ezrin was kept at 4°C in a buffer containing 70 mM NaCl, 25 mM 2-(*N*-morpholino)ethanesulfonic acid (MES) at pH 6.2 (MES-NaCl buffer). For experiments with GUVs, the buffer was brought to pH 7.4 with 30 mM Tris (Ezrin buffer). Vesicles were prepared in a buffer containing sucrose (165 mM sucrose, 2 mM Tris, 0.5 mM EGTA, pH = 7.4, sucrose buffer) and were resuspended in a glucose buffer (170 mM glucose, 2 mM Tris, 0.5 mM EGTA, pH = 7.4, glucose buffer). The osmolarities of the buffers were checked using an osmometer (Vapro, Wescor, Logan, UT). We measured the following osmolarities: (173 ± 3) mOsm for the sucrose buffer, (180 ± 3) mOsm for the glucose buffer, and (184 ± 3) mOsm for the ezrin buffer.

Protein expression, purification, and labeling

The expression and purification of wild-type (WT) ezrin cloned in the pGEX 2-T vector have already been described (31). Recently, we produced ezrin with an additional cysteine at its C terminus following two extra glycine residues (GGC) to covalently couple it to a maleimide fluorophore (22). Both wild-type ezrin and ezrin-cysteine were obtained using the same purification procedure. Labeling of ezrin-cysteine was carried out using either Alexa488-C5-maleimide (Alexa488) or Alexa546-C5 maleimide (Alexa546), both from Molecular Probes. Purified ezrin conserved in the MES-NaCl buffer

TABLE 1 Summary of the studies investigating protein interactions with PIP_2-containing GUVs prepared by the gentle hydration method or by electroformation

Study	GUVs preparation	Composition	Suspending medium	Proteins
Gentle hydration				
Takeda et al. (27)	25°C in 5 mM Tris-HCl	PC/PE/PG/PIP_2	KCl buffer (0–120 mM)	Talin
Tong et al. (51)	37°C in 100 mM sucrose	DOPC/DOPG/SM/Chol/PIP_2/TMR-PIP_2	100 mM glucose	GAP-43
Golebiewska et al. (28)	35–40°C in 100 mM KCl	POPC/PS/PIP_2	100 mM KCl	MARCKS (151-175)-Alexa488
Heuvingh et al. (45)	in 280 mM sucrose	DOPC/PIP_2	HeLa cell extracts	ARF1, Actin
Electroformation				
Liu and Fletcher (13)	60°C in 350 mOsm sucrose	DOPC/DPPC/Chol/TMR-PIP_2/PIP_2	50 mM KCl	N-WASP, Arp2/3, Actin
Gokhale et al. (14)	60°C in deionized water	POPC/POPE/POPS/PIP_2	160 mM NaCl	Annexin 2
Moens et al. (29)	45°C in 200 mM sucrose	POPC/PIP_2/TMR-PIP_2 (or FL-PIP_2, both C6)	200 mM glucose	Profilin

PC, phosphatidylcholine; POPC, 1-palmitoyl-2-oleoyl-*sn*-glycero-3-phosphatidylcholine; PE, phosphatidylethanolamine; POPE, 1-palmitoyl-2-oleoyl-*sn*-glycero-3-phosphatidylethanolamine; PG, phosphatidylglycerol; DOPG, dipalmitoylphosphatidylglycerol; SM, sphingomyelin; PS, phosphatidylserine; POPS, 1-palmitoyl-2-oleoyl-*sn*-glycero-3-phosphatidylserine; DPPC, dipalmitoylphosphatidylcholine.
All experiments were carried out at physiological pH (7–7.4).

was treated with a 10-fold molar excess of Alexa488-C5-maleimide or Alexa546-C5 maleimide (dissolved in DMSO) for 90 min at room temperature in MES-NaCl buffer. The labeling reaction was subsequently quenched by adding an excess amount of dithiothreitol and the labeled protein was separated from the reagents using a Sephadex G25 column (GE Healthcare, Velizy, France) eluted with the MES-NaCl buffer. The labeling efficiency of ezrin was estimated by determining the respective molar concentration of dye and of protein and calculating the grafting ratio (molar extinction coefficients are respectively: $\varepsilon = 72{,}000\ M^{-1}\ cm^{-1}$ for Alexa488 at 495 nm, $\varepsilon = 104{,}000\ M^{-1}\ cm^{-1}$ for Alexa546 at 544 nm, $\varepsilon = 69\ 000\ M^{-1}\ cm^{-1}$ for ezrin at 280 nm). Under our labeling conditions, ~0.93 mol of Alexa488 and ~0.92 mol of Alexa546 were incorporated per mol of ezrin.

GUVs and LUVs

GUVs were prepared using the electroformation method first described by Angelova et al. (32). The vesicles were formed using DOPC or DOPC and cholesterol (15%), with various amounts of PIP_2 (from 1% to 10% in weight). Briefly, 20 μL of lipid mixture at 2.5 mg/mL in chloroform/methanol 2:1 (v/v) were spread on two ITO-coated plates and quickly dried under nitrogen flow. The slides were placed under vacuum for 2 h to remove traces of organic solvent. After solvent evaporation, an electroformation chamber was formed using the ITO plates (their conductive sides facing each other), a rubber ring, and Vitrex paste to seal the chamber. The chamber was filled with ~1.5 mL of sucrose buffer and placed in an incubator at 38°C. A function generator was used to apply an AC voltage at 10 Hz, the voltage being progressively increased from 200 mV to 1 V within 30 min and kept constant for the remaining 45 min. Vesicle detachment was then achieved by decreasing the frequency to 5 Hz for 15 min. GUVs were stored at room temperature.

LUVs were prepared as described previously (22). Briefly, the appropriate lipid mixture was dried in a Speedvac rotary evaporator overnight, and the lipids were rehydrated in the sucrose buffer for 2 h at 37°C (interrupted by rigorous vortexing every 15 min), then extruding the multilamellar vesicles through a stack of two polycarbonate filters (100 nm pore size diameter) using the mini-extruder from Avanti Polar Lipids. Final concentrations of lipids were measured using the Phospholipid B kit (Wako Chemicals GmbH, Neuss, Germany) and were within 90–95% of the expected concentration. LUVs were stored at room temperature at 10 mg/mL lipid concentration.

Light and confocal microscopy observations

For microscopy observations, GUVs were let to sediment in a glucose buffer with a weakly higher osmolarity than the sucrose buffer such as to slightly deflate the GUVs and render them more flaccid and fluctuating. The observation chambers were pegylated to prevent attractive interactions between GUVs and the glass substrate (22). A silicone insulator (P24742, Molecular Probes) glued to the pegylated glass slides was used to prepare several wells, which were filled with 15 μL of sample. Experiments with the PIP_2 antibodies were carried out in the ezrin buffer. For the experiments with the protein, GUVs were diluted 1:10 in the ezrin solution. Ezrin total concentration was in the range 14–22 μM. Confocal microscopy observation of GUVs were carried out on a spinning disk rapid confocal imager Ultra view ERS (Perkin Elmer, Courtaboeuf, France) with a 63× oil objective (NA = 1.4).

Image analysis

Fluorescent images were analyzed with ImageJ software (http://rsb.info.nih.gov/ij/). Image superposition was realized by using the «rgb merge» function of Image J. Using the plug-in «Radial Profile plot», the integrated intensities along concentric circles (centered at the center of the GUVs) were measured. For experiments with nonfluorescent GUVs immersed in an ezrin solution containing fluorescently labeled ezrin, the integrated intensity I was normalized such that the resulting intensity, I_{NORM}, was equal to 0 in the interior of the GUV (where the measured intensity I_{INT} was the noise signal) and equal to 1 in the external medium (I_{EXT}, where the measured intensity is the background intensity of the ezrin medium). Hence, the normalized intensities were calculated following $I_{NORM} = (I - I_{INT})/(I_{EXT} - I_{INT})$.

To quantify the heterogeneous nature of the membrane of GUVs, we adapted a recently published procedure (33). The principle is that the formation of clusters leads to an increased occurrence of areas with high (cluster) and low (intercluster) fluorescence intensities. Therefore, cluster formation results in increased SD of the fluorescence signal. The plug-in «Oval Profile Plot» was used to extract an azimuthal profile of the equatorial section of a GUV (along all the GUV contour length, i.e., for 360°). The profiles along the membrane contour were obtained by measuring over a circular region 5 pixels thick, to reduce the noise. The mean fluorescence intensity along the GUV contour was deduced (I_{MEAN}) as well as its SD (σ). To compare different GUVs, the ratio, σ/I_{MEAN}, is given and expressed in percentage. Thus, for one experimental condition, this ratio calculated over several GUVs quantifies the heterogeneity of the membrane. The lowest it is, the more homogeneous is on average the membrane of GUVs obtained in a given experimental condition. The lowest ratio was measured to be $\sigma/I_{MEAN} = (8.7 \pm 1.1)$ % (see Fig. 4 *A*) and thus, clusters were defined as areas of membrane with intensities 15% higher than I_{MEAN}.

ζ-Potential measurements

The average ζpotential of the vesicles was measured on a Malvern Zeta Sizer NanoZS (Malvern, Worcestershire, United Kingdom). The electrophoretic mobility of GUVs (respectively LUVs) was measured at 0.05 mg/mL lipid concentration (respectively 0.1 mg/mL) in the sucrose buffer and the ζ-potential, ξ, of a vesicle, which is the electrostatic potential at the shear plane, was calculated using the Helmholtz-Smoluchowski equation (34), $\xi = (u\eta/\varepsilon_R\varepsilon_0)$, where u is the velocity of the vesicle in a unit electric field (between 50 and 150 $V.cm^{-1}$ for this configuration); η is the viscosity of the aqueous solution; ε_R is the dielectric constant of the aqueous solution; and ε_0 is the permittivity of free space. The ζ-potential is proportional to the surface charge density (34). Numerical results are given as (mean ± SD). For each measurement, 750 μL of the GUV suspension were introduced in the measurement cell. Three measurements were carried out for each sample from at least two independent preparations. In fact, the SD on each measurement, as given by the apparatus, were ~12% for GUVs and range from ~18% to ~100% for LUVs (higher SD when the potential was close to 0) and were higher than the reproducibility of the measurement, which is of the order of 5% (for a given sample as well as for independent samples). Thus we plot as error bars in the graph the SD for each measurement. The maximum size of the vesicles that can be measured is ~10 μm. To avoid sedimentation of the GUVs, ζ-Potential measurements were carried out with GUVs suspended in the sucrose buffer. For the sake of comparison, the same buffer was chosen for the measurements on LUVs.

RESULTS

ζ-Potential of GUVs

In a first step, we investigated the insertion of PIP_2 in membranes composed uniquely of DOPC or composed of a mixture of DOPC and cholesterol (weight fraction, 15%), as cholesterol has been reported to strengthen membranes (35,36), and consequently to increase the stability and integrity of liposomes (37). GUVs were thus electroformed with increasing percentages of PIP_2 in the initial lipid mixture, in the presence or in the absence of cholesterol. The ζ-potential measurements were carried out within 2 h after GUVs preparation (time T0) or 24 h after their preparation. Fig. 1, *A* and *B* show the ζ-potential for DOPC and DOPC/Chol GUVs, with various amounts of PIP_2. For DOPC/PIP_2

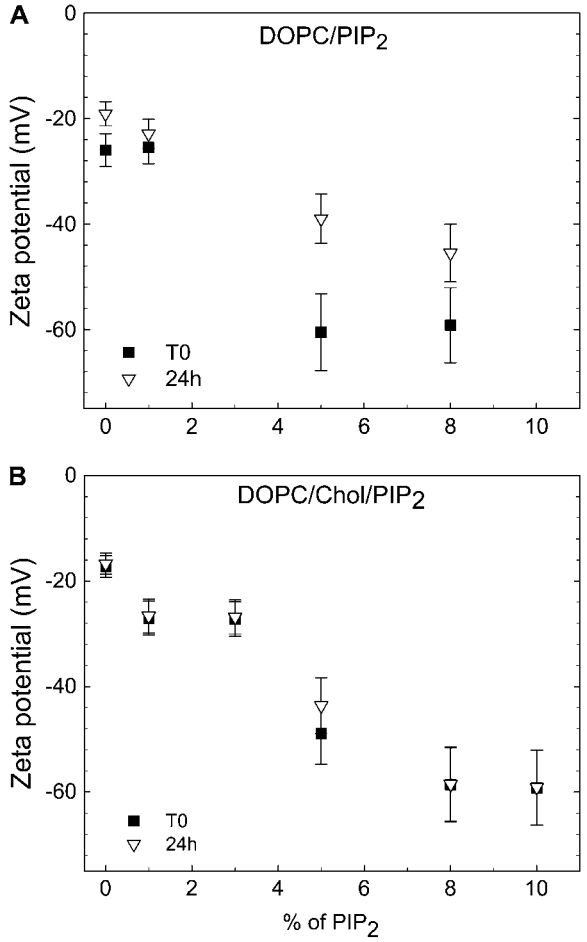

FIGURE 1 ζ-Potential of giant unilamellar vesicles (GUVs) as a function of the mass percentage of PIP_2 incorporated in the initial lipid mixture. The electrophoretic mobility of GUVs composed of either DOPC/PIP_2 (*A*) or DOPC/Chol/PIP_2 (*B*) was measured and the ζ-potential was calculated as explained in the text, after the preparation of the GUVs (time T0) or 24 h after their preparation. Values are (mean ± SD) of the measurement.

GUVs, we observe that the initial ζ-potential decreases as the percentage of PIP_2 increases but reaches a plateau at ~5% in PIP_2 (Fig. 1 *A*). We find, however, noticeable differences between the values measured within 2 h after GUVs electroformation (T0) and 24 h later, indicating that the DOPC/PIP_2 GUVs may evolve during the storage period. In fact, the ζ-potential of GUVs tends to rise with time as if PIP_2 was leaking from the GUV membrane. For DOPC/Chol/PIP_2 GUVs, similarly to the GUVs without cholesterol, the ζ-potential decreased steadily when PIP_2 concentration is increased (Fig. 1 *B*), which suggests that more and more PIP_2 molecules are effectively incorporated in the membrane of GUVs. A plateau in ζ-potential is reached for PIP_2 percentages higher than 8%. Interestingly, and in sharp contrast to the GUVs without cholesterol, the GUVs containing cholesterol seem to be stable over a duration of 24 h as their ζ-potentials remain almost identical after 1 day in the storage buffer (sucrose buffer). We also noticed that repeated measurements on GUVs made from a lipid mixture containing 15% of cholesterol and 10% PIP_2 lead to an increase in the potential after five measurements have been carried out, which suggests that GUVs containing high amounts of PIP_2 are more fragile and might be more easily electroporated (38). This effect was not observed when the PIP_2 weight fraction of the initial lipid mixture was decreased to 5%.

Thus, in the following, the total PIP_2 percentage was fixed at 5% as the GUVs were stable in these conditions (no evolution of the ζ-potential over repeated measurements).

Comparison of PIP_2-containing GUVs with PIP_2-containing LUVs and with POPS-containing GUVs

As LUVs have been most often used as biomimetic systems to investigate PIP_2/protein interactions (10,14,15), we compared the ζ-potential of GUVs made by electroformation to that of LUVs made by a rehydration method followed by extrusion through a calibrated porous membrane, for the same initial lipid compositions (Fig. 2 *A*). One finds that the ζ-potential, ξ, of GUVs and of LUVs follows the same trend: ξ decreases steadily on increase of the mass percent of PIP_2 in the initial lipid mixture. The ζ-potential of LUVs is related linearly to that of GUVs with a slope of 0.86 (Fig. 2 *B*). Thus, GUVs and LUVs can be considered to be similar in terms of PIP_2 insertion. However, the potentials of GUVs is systematically found lower than that of LUVs. We note that this difference is observed even in the absence of PIP_2. Indeed we measured $\xi \sim (-17.2 \pm 2.0)$ mV for DOPC/Chol GUVs and $\xi \sim (-6.9 \pm 6.3)$ mV for DOPC/Chol LUVs. These negative values might be partly attributed to an effect of the buffer (sucrose buffer without salt). In addition, the difference between LUVs and GUVs might arise from the fact that GUVs have a ~100× larger diameter than LUVs, which makes them more deformable when placed in an electric field (39). Indeed, a prolate deformation of a GUV would presumably decrease the drag force acting on the GUV; hence this would increase its mobility, leading to an apparent larger surface density and thus a more negative potential. Furthermore, the deformation of GUV may depend on the charge density of the GUV: a GUV that possesses a higher charge density will presumably deform more than a GUV with a weaker charge density. Hence, we would expect the difference between the ζ-potential of GUVs and that of LUVs to increase when the % of PIP_2 increases, as observed experimentally (Fig. 2 *A*).

POPS is often used as negatively charged lipid to mimic the composition of the inner plasma membrane, either alone or in combination with PIP_2 (10,26). In addition, POPS has been reported to bind nonspecifically to many types of proteins, including MARCKS (40) and the matrix protein of vesicular stomatitis virus (41). Thus, POPS-containing GUVs prove as a useful control to check for nonspecific electrostatic interactions between a protein and a negatively charged lipidic membrane. The ζ-potential of GUVs fabricated from a

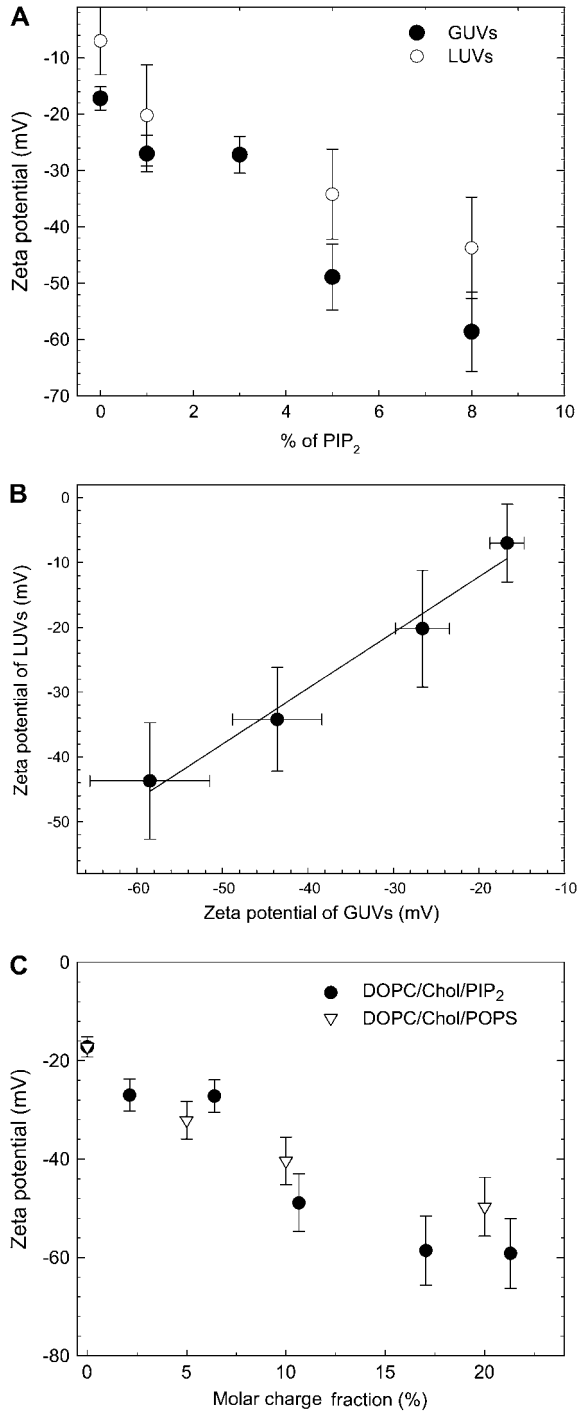

FIGURE 2 Comparison of GUVs with LUVs and of PIP_2-GUVs with POPS-GUVs. (*A*) ζ-Potential of GUVs as compared to that of LUVs with the same initial lipid mixture (DOPC/Chol/PIP_2) with various amounts of PIP_2. (*B*) ζ-Potential of LUVs plotted as a function of that of GUVs for a given % of PIP_2 in the initial lipid mixture for measurement made at 24 h (same data as in Fig. 2 *A*). The linear regression has a slope of 0.86. (*C*) ζ-Potential of GUVs electroformed from a lipid mixture containing increasing percentages of PIP_2 as compared to that of GUVs electroformed from a lipid mixture containing increasing percentages of POPS. For direct comparison, the data have been plotted on the same *x* axis as a function of the molar charge density, considering that each POPS molecule possesses one charge and each PIP_2 molecule possesses three charges.

lipid mixture composed of DOPC, cholesterol and various amounts of POPS (up to 20% in weight) have been measured. Similarly to our findings with PIP_2, we measured that the ζ-potential decreases as the amount of POPS increases. It has been reported that PIP_2 has a net charge of -3 and that POPS has a net charge of -1 (20). Therefore, to directly compare the results obtained with PIP_2 and with POPS, we have plotted in Fig. 2 *C* the two sets of data as a function of the molar charge fraction of the initial lipid mixture. Both sets of data are in good agreement and fall over a unique curve. On the one hand, this indicates that the approximation of one PIP_2 equals 3 POPS (as far as the electric charge is concerned) is valid. On the other hand, this confirms the similar incorporation of POPS and PIP_2 in the membrane of GUVs prepared by electroformation. This is consistent with our observation that a saturation of the ζ-potential is measured for mass fraction of PIP_2 $>8\%$ (Fig. 1 *B*). In all cases, a limit to the incorporation of negatively charged lipids into GUVs made by electroformation seems to be set to a molar charge fraction of $\sim 20\%$, hence a mass fraction of PIP_2 of the order of 8% (Fig. 2 *C*), whereas up to 20% of PIP_2 can be incorporated in LUVs without evidence for a saturation of the ζ-potential (22). This finding is in agreement with previous reports that show that GUVs cannot be formed by electroformation from a lipid mixture containing 20% POPS (25).

Visualization of PIP_2 in the membrane of GUVs

The effective incorporation of fluorescent PIP_2 can be qualitatively observed using BODIPY-labeled PIP_2. Fluorescent long-chain (C16) PIP_2 analogs were used in this study because our initial attempts to insert the short-chain (C6) BODIPY labeled PIP_2 were always unsuccessful for both TMR- and FL-PIP_2. Moreover, we noticed that the long chain ones did not incorporate into the GUVs membrane by electroformation when experiments were carried out at 25°C but were incorporated when carried out at 38°C (Fig. 3, *A* and *B*). Finally, TMR-PIP_2 was systematically found to exhibit a preferential orientation in the membrane of GUVs, as shown by a modulation linear with the square of the angle sine of the azimuthal intensity, when the GUVs were observed with the linearly polarized light of the laser of the confocal microscope (42) (Fig. 3 *B*). A modulation of the intensity was never observed for FL-PIP_2 (Fig. 3 *A*). This difference has presumably to be attributed to the more hydrophobic and less flexible fluorescent dye of the TMR-PIP_2 molecule than that of the FL-PIP_2 molecule, which results in a more ordered insertion of the TMR-PIP_2 molecule in the lipid bilayer. Noticeably, when TMR-PIP_2 micelles were added to a suspension of GUVs formed previously, TMR-PIP_2 incorporated spontaneously the membrane of the GUVs, whereas unlabeled PIP_2 (as checked with PIP_2 antibodies) or FL-PIP_2 did not, as checked with PIP_2 antibodies-labeling (data not shown).

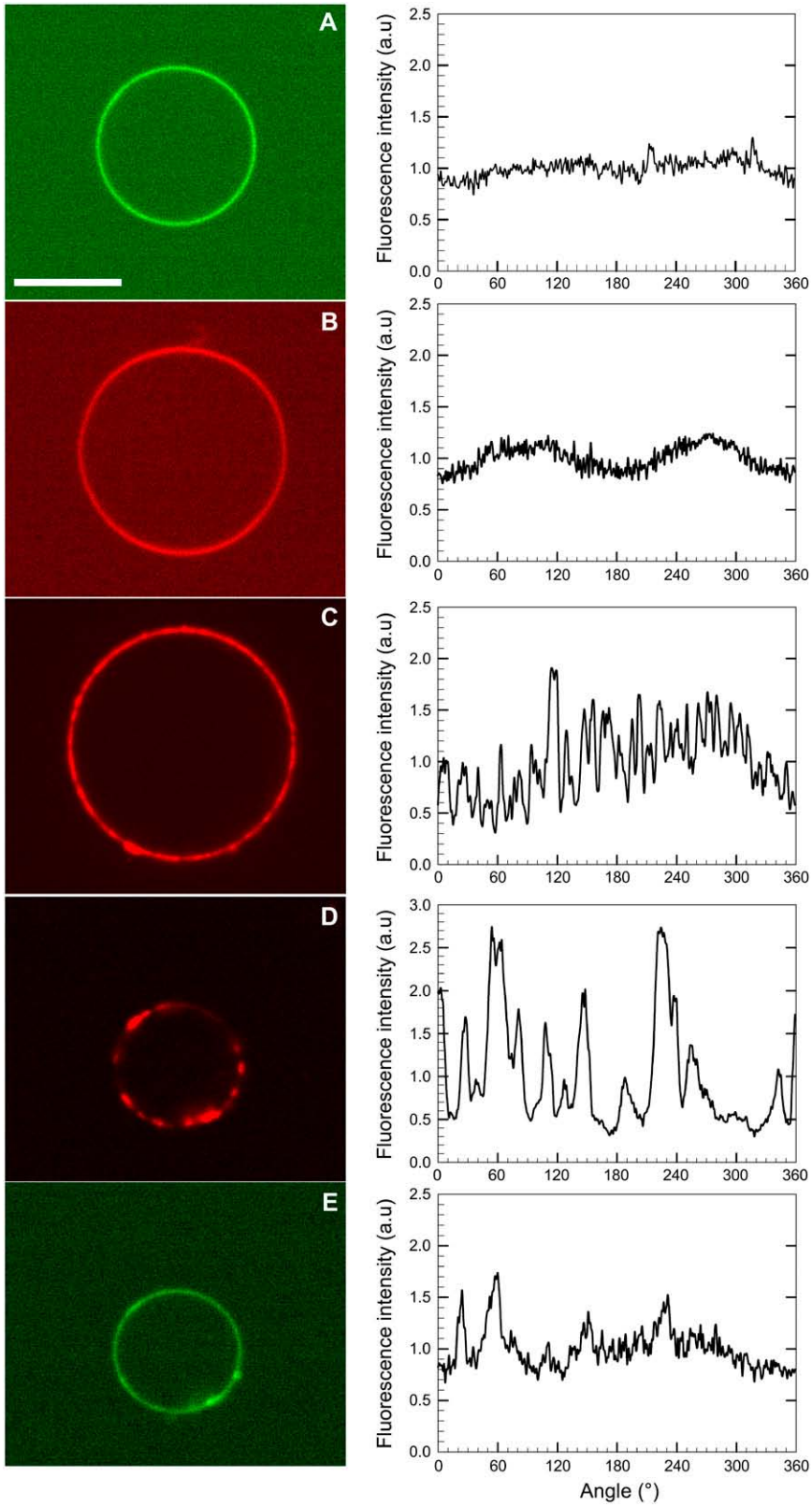

FIGURE 3 Confocal microscopy observations of PIP_2 insertion in GUVs. (*A* and *B*) Direct observation of the GUVs by insertion (*A*) of 0.1% FL-PIP_2 (C16) in the initial lipid mixture, DOPC/Chol/PIP_2/FL-PIP_2 80:15:4.9:0.1, (*B*) of 0.1% TMR-PIP_2 (C16) in the initial lipid mixture, DOPC/Chol/PIP_2/TMR-PIP_2 80:15:4.9:0.1. Indirect observation of PIP_2-containing GUVs (DOPC/Chol/PIP_2, (80:15:5) by immunolabeling with PIP_2 secondary (*C*) and tertiary (*D*) antibodies. In (*C*), RAM-Alexa 568 secondary fluorescent antibodies were used. In (*D*), unlabeled goat anti-mouse antibody (GAM) followed by donkey anti-goat antibodies (tertiary antibodies) coupled to Alexa 488 (DAG-Alexa 488) were used. (*E*) Direct observation of FL-PIP_2 for the same GUVs as (*D*) (composition similar to *A*). Scale bars: 10 μm. On the right hand side of the images, the corresponding fluorescence intensity profiles along the GUV contour are plotted.

Noticeably, the membrane of GUVs labeled with FL-PIP_2 appears homogeneous without clusters. We measured $\sigma/I_{MEAN} = (9.8 \pm 1.9)$ % in the sucrose buffer, and $\sigma/I_{MEAN} = (8.7 \pm 1.2)$ %, in the ezrin buffer. Hence, in the following, σ/I_{MEAN} of the order of 10 was taken as the reference value for a homogeneous labeling.

We also verified that the ζ-potential of GUVs made from a lipid mixture containing 4.9% of unlabeled PIP_2 and only a trace (0.1%) of fluorescent FL-PIP_2 ($\xi = (-47.3 \pm 5.6)$ mV) was close to that of GUVs made from a lipid mixture containing only 5% of unlabeled PIP_2, ($\xi = (-48.9 \pm 5.9)$ mV). This indicates that the 0.1% of fluorescent lipid inserted in the membrane does not contribute to the overall potential, as expected. It is important to note that TMR-PIP_2 and FL-PIP_2 are used here as tracers. Thus, only a very small fraction of % of these lipids (<0.5%) is required to visualize the membrane. Indeed, the limit of self-quenching of these lipids is ~1% of TMR-PIP_2 (26) and 0.8% for BODIPY FL-PIP_2 (Fig. S2 in Supplementary Material, Data S1), as determined by fluorescence spectroscopy of LUVs containing increasing percentages of FL-PIP_2.

Thus, in the following, the total PIP_2 percentage was fixed at 5% as the GUVs and when fluorescent PIP_2 was used, it was always added at 0.1% (2% of the total amount of PIP_2).

Alternatively, it is possible to visualize the presence of PIP_2 in the membrane by labeling it with primary antibodies against PIP_2 and then secondary antibodies coupled to a fluorescent dye (Fig. 3 *C*), or with unlabeled secondary antibodies followed by labeled tertiary antibodies, to build larger complexes (Fig. 3 *D*). We observed in this case the presence of patches for labeled antibodies, an aspect with was never observed for direct insertion of fluorescent PIP_2 (Figs. 3, *A* and *B*, and 4). More quantitatively, $\sigma/I_{MEAN} = (8.7 \pm 1.1)$ %, for FL-PIP_2-labeling in the absence of PIP_2 antibodies (Fig. 3 *A*), $\sigma/I_{MEAN} = (27.4 \pm 6.5)$ % for fluorescent secondary antibodies (Fig. 3 *C*), and $\sigma/I_{MEAN} = (44.9 \pm 14.9)$ % (Fig. 3 *D*) for fluorescent tertiary antibodies (Fig. 4, *three first columns*). Noticeably, when FL-PIP_2 was observed in the GUVs in contact with the tertiary antibodies, the membrane of the GUVs appears more homogeneous than when the fluorescence of the tertiary antibodies is measured (Fig. 3, *E* and *D*). We found $\sigma/I_{MEAN} = (19.5 \pm 7.5)$ % for FL-PIP_2 direct visualization, whereas $\sigma/I_{MEAN} = (44.9 \pm 14.9)$ % tertiary antibodies visualization (Fig. 4, *4th column*). Hence the apparent heterogeneous character of the membrane of the GUV increases with the size of the detection molecule: fluorescent secondary antibodies might induce some PIP_2 clustering, which is enhanced when larger anti-PIP_2 complexes (unlabeled secondary antibodies followed by the addition of fluorescent tertiary antibodies) are used. However, direct visualization of fluorescent PIP_2 and indirect visualization through antibodies, provide quantitatively different results for clustering effects, which suggest that the clustering effect visualized via antibodies is essentially artifactual.

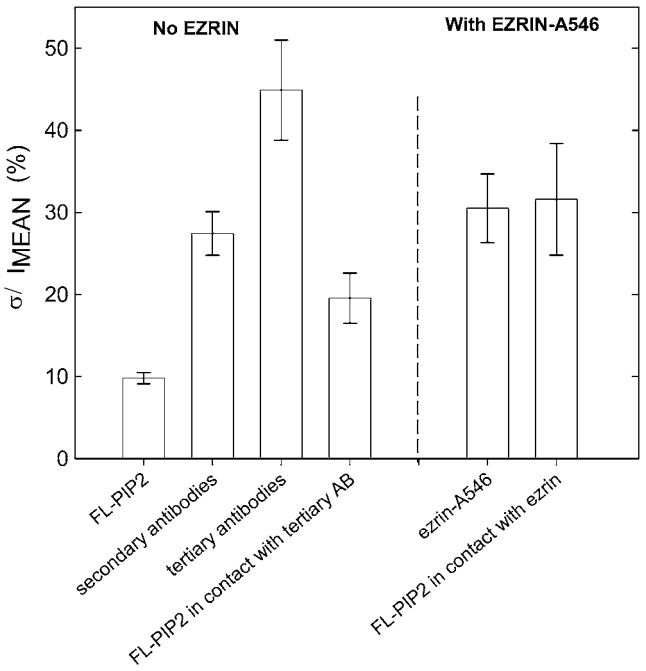

FIGURE 4 Analysis of the heterogeneities in the GUV membranes. The ratio of the SD of the fluorescence signal along the GUV membrane divided by the mean intensity of the GUV membrane (σ/I_{MEAN}) is given as mean ± SE for all the GUVs analyzed. The first four columns correspond to experiments carried out in the absence of ezrin in the following order: labeled PIP_2-GUVs using direct labeling or indirect labeling with secondary and tertiary antibodies, (columns 1, 2, and 3, respectively). Column 4 is the observation of FL-PIP_2 GUVs labeled with tertiary antibodies (observation in the green channel whereas antibodies are observed in the red channel). The last two columns correspond to images taken in the presence of ezrin in solution: in this case, either ezrin-Alexa546 (column 5) or FL-PIP_2 (column 6) were observed. All these experiments were carried out in the ezrin buffer.

Stability of GUVs in physiological medium and in the presence of divalent ions

First, we verified that the size distribution of GUVs made from a lipid mixture containing 5% PIP_2 was not different from that of pure DOPC/Chol vesicles. The median diameter was 8 μm for GUVs without PIP_2 and 9 μm for GUVs with PIP_2, as evaluated by analyzing more than 160 GUVs for each condition. As the GUVs prepared by electroformation were suspended in a sucrose solution, a transfer in a physiological medium was necessary if the GUVs had to be used for protein/membrane studies (13,14). Therefore, we took care that the osmolarity of the ezrin buffer into which the GUVs could eventually be resuspended, (184 ± 3) mOsm was slightly higher than that of the initial sucrose buffer, (174 ± 3) mOsm, so that the GUVs were always slightly deflated and therefore fluctuating (43). The transfer into a salty medium may render the GUVs more fragile and with time could induce some defects, in particular because of the existence of a transmembrane electric potential. However, we measured for FL-PIP_2- labeled GUVs that $\sigma/I_{MEAN} = (9.8 \pm 1.9)$ % in the sucrose buffer, (8.7 ± 1.1) % just after immersion in the ezrin

buffer, and (9.7 ± 2.1) % after 2 h in this buffer. Thus, the immersion in the ezrin buffer did not affect the homogeneity of the GUV membrane.

In view of the investigation of biological phenomena, it is crucial to quantify the stability of GUVs when put into contact with divalent cations like Ca^{2+} and Mg^{2+} as these ions are important in many physiological processes, including interaction of several proteins, including annexin 2 with membranes (14) and polymerization of actin (44). Indeed, these ions have been reported to interact with the phosphate groups of PIP_2 (20). Thus, we investigated the contact of these ions with PIP_2-containing GUVs and labeled with FL-PIP_2. Before contact, the vesicles exhibited a homogenous PIP_2 distribution (Fig. 3 *A*). However, low amounts of Mg^{2+} and Ca^{2+} (for concentrations >25 μM for Ca^{2+} and >300 μM for Mg^{2+}) induced the formation of clusters leading to $\sigma/I_{MEAN} > 20\%$ (Fig. 5, *A–C*). Interestingly, these clusters or aggregates could only be observed in fluorescence microscopy and were not visible by differential interference contrast microscopy, which indicates that the formation of these clusters is neither associated to a shape change of the GUVs nor to a visible aggregation of the lipid membrane, but only to PIP_2 aggregation. When the ions concentrations were higher (>300 μM for Ca^{2+} and >1 mM for Mg^{2+}), vesicles rupture within 10 min was also observed. We have plotted in Fig. 5 *C* σ/I_{MEAN} as a function of the concentration of divalent ions in the external medium (analysis was carried out 10 min after addition of the ions). We found that, for both ions, the heterogeneity of the GUVs increases steadily. Fig. 5 *C* also shows that GUVs were more sensitive to Ca^{2+} than to Mg^{2+}.

PIP_2-containing GUVs interact with ezrin

We subsequently investigated the interactions of the PIP_2-containing GUVs with ezrin, a protein that possesses a FERM domain at its N-terminal and interacts with lipid membranes via that domain. Indeed, ezrin has already been shown to interact with PIP_2-containing SLBs (12), with PIP_2-containing LUVs (22), and with giant vesicles made by the gentle hydration method (27).

The PIP_2-containing GUVs (composition of the initial lipid mixture DOPC/Chol/PIP_2, 80:15:5) were introduced in a chamber containing ezrin, with a concentration in the range of 14–22 μM. Such high concentration of ezrin was chosen to ensure that a large amount of protein was available for lipid binding, as the affinity of ezrin to PIP_2-LUVs was found to be ~ 5 μM (22) (see details in Data S1). We observed that ezrin localized at the membrane of GUVs only in the case where PIP_2 was inserted in the membrane (Fig. 6 *B*). When PIP_2 was replaced by POPS introduced at a higher percentage (15%) as a negative control (Fig. 6 *C*), the membrane of GUVs was never labeled, similarly to what was observed with pure DOPC/Chol GUVs (Fig. 6 *A*). The mean radial concentration profile of ezrin (calculated for 14 GUVs in each condition) quantifies the increase of ezrin concentration in the close vicinity of the membrane of GUVs when their membrane appeared labeled (Fig. 6 *D*). The fluorescence intensity of the ezrin-labeled GUVs membrane was at most 1.94 times higher than the fluorescence of the exterior, indicating that the local

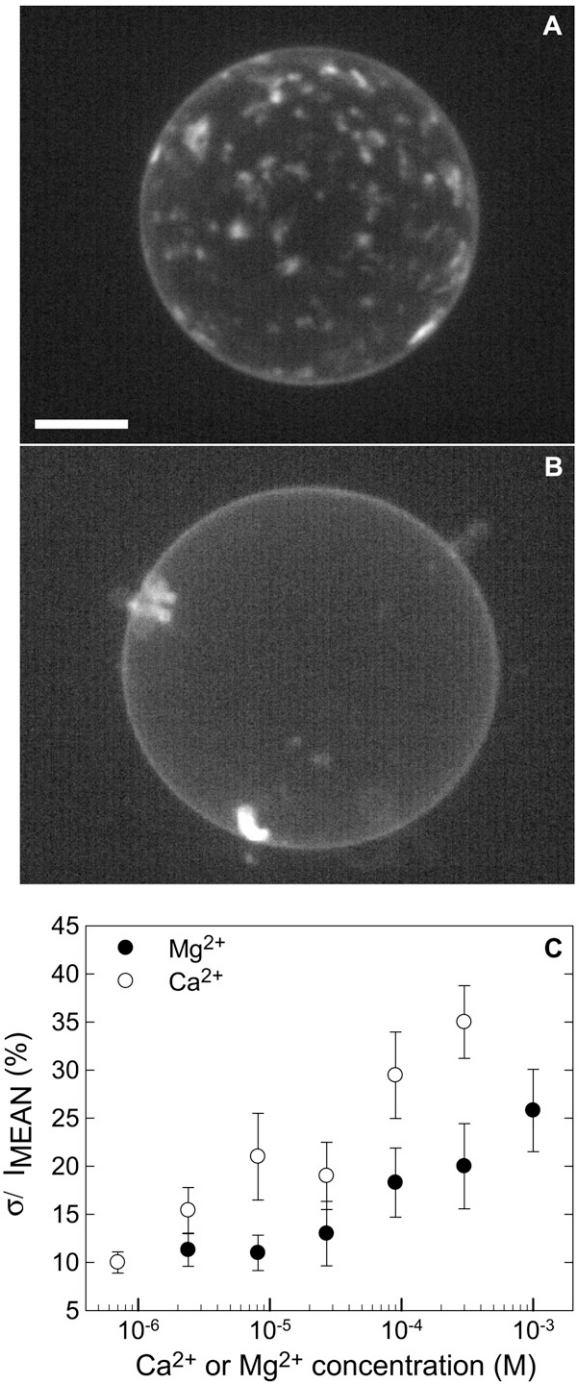

FIGURE 5 Effect of divalent ions on PIP_2-containing GUVs (composition of the initial lipid mixture DOPC/Chol/PIP_2/FL-PIP_2, 80/15/4.9/0.1). Projections of a stack of images taken by confocal microscopy at different height of GUVs in the glucose buffer (*A*) with 90 μM Ca^{2+}; (*B*) with 90 μM Mg^{2+}; (*C*) (σ/I_{MEAN}) for the GUVs as a function of the Ca^{2+} and Mg^{2+} concentration in solution. Scale bar: 10 μm.

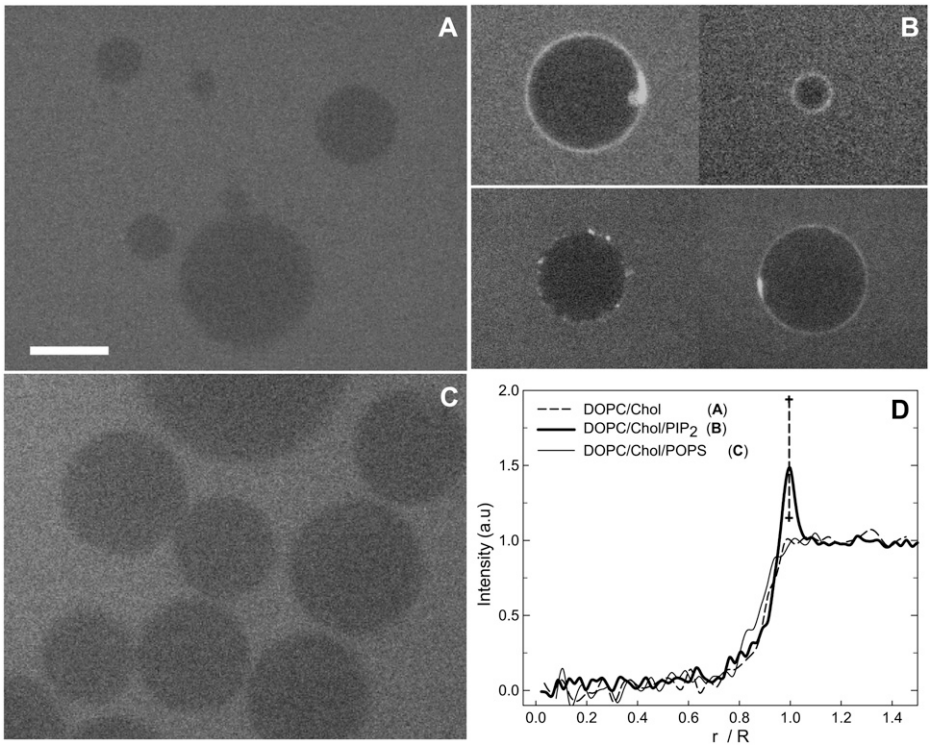

FIGURE 6 Contact between GUVs and ezrin (mixture containing 15 μM of WT ezrin and 200 nM of ezrin-Alexa488). (*A*) GUVs composed only of DOPC and cholesterol (DOPC/Chol 85:15). (*B*) GUVs containing PIP_2 (DOPC/Chol/PIP_2, 80:15:5). (*C*) GUVs containing POPS as negatively charged lipid (DOPC/Chol/POPS, 70:15:15). (*D*) The radial concentration profiles of ezrin for the three different types of GUVs are represented after normalization (the distance r from the center of the GUV is normalized by the radius of the vesicle R; the fluorescence intensity is normalized such as it is equal to 0 inside the GUV and 1 in the external medium.). Each profile represents the mean of 14 different profiles from individual GUVs. The dotted vertical line shows the range of values measured for the height of the peak (between 1.15 and 1.94). The scale is the same for the three pictures. Scale bar: 10 μm.

ezrin concentration is roughly twice the concentration in the bulk at most. We noticed that 23% of the GUVs were labeled at their membrane (four independent experiments, 341 GUVs observed in total), whereas for POPS, <1% were labeled (Table 2). Similar percentages of labeled GUVs were observed for GUVs containing unlabeled PIP_2 with or without 0.1% of FL-PIP_2 (Table 2). This shows that FL-PIP_2 does not change the interaction properties of ezrin with PIP_2-containing GUVs. At present, there are only few quantitative studies published on GUVs interacting with proteins. When a thorough quantification of the images is carried out, the percentages measured for other proteins interacting with PIP_2-containing GUVs (27,45) fall in the range of what is observed in this study. When GUVs were made from a initial lipid mixture containing only DOPC and PIP_2 (DOPC/PIP_2 95/5) without cholesterol, this percentage fell to 7% (three independent experiments, 208 GUVs counted) that might be related to the highest and less stable ζ-potential values obtained for these latter GUVs, as if PIP_2 was incorporated in smaller quantities or these membranes were less stable.

Importantly, we also verified that ezrin-Alexa488 and ezrin-Alexa546 exhibited a similar behavior that did not depend on the dye properties (Fig. 7). This is an important point as recent experiments using a peptide (MARCKS 151-175) labeled with either Alexa488 (a rather hydrophilic moiety) or Texas Red (a more hydrophobic moiety) showed that the Texas Red labeled peptide did permeate the membrane of GUVs (membrane composition PC/PS/PIP_2: 70:30:0.1) and was mostly located inside the GUVs whereas Alexa488 labeled peptide did not permeate the membrane of GUVs (26). These different observations are probably related to the different size of the two proteins, ezrin being indeed much larger than the MARCKS(151–175) peptide (24 amino acids for the peptide versus 586 for ezrin) as well as to the mode of interaction (electrostatic for MARKS, stereospecific for ezrin). In our case, we also confirmed that the percentage of labeled GUVs did not depend on the type of

TABLE 2 Quantification of the number of ezrin-labeled GUVs and of the presence of clusters for GUVs of different composition

GUV composition	Ezrin-labeled GUV (in % of the total GUVs)	Presence of clusters (in % of labeled GUVs)
Ezrin-Alexa488		
DOPC/Chol, 85:15 (n = 222)	0	-
DOPC/Chol/POPS, 70:15:15 (n = 90)	<1	-
DOPC/PIP_2, 95:5 (n = 208)	7	79
DOPC/Chol/PIP_2 80:15:5 (n = 537)	23	79
Ezrin-Alexa546		
DOPC/Chol/PIP_2/FL-PIP_2 80:15:4.9:0.1 (n = 51)	22	Visualization of ezrin-Alexa546:81 Visualization of FL-PIP_2:90

Clusters were defined as areas with intensities 15% higher than the mean GUV intensity along the contour length. n is the number of GUVs considered.

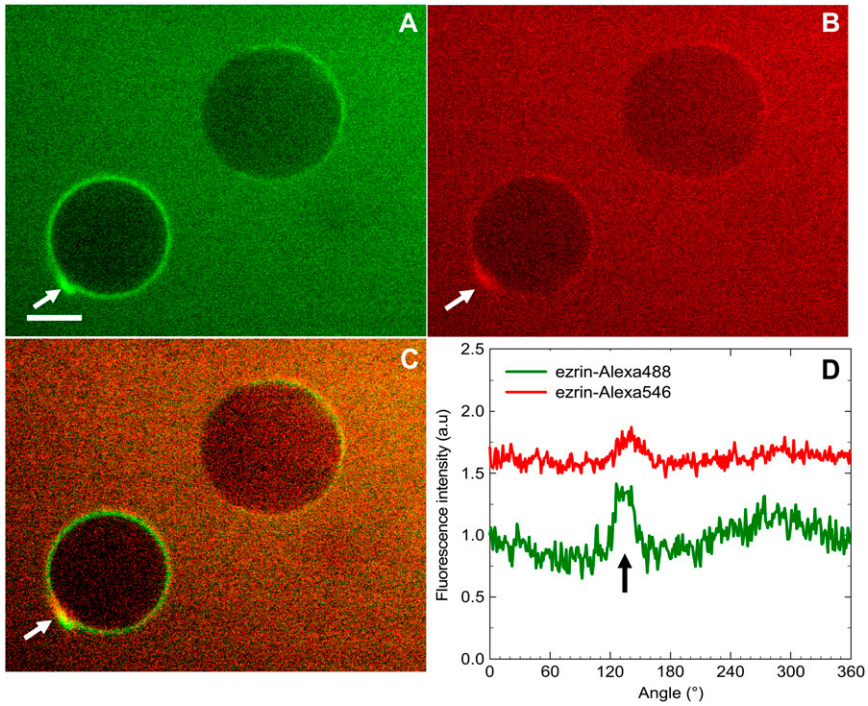

FIGURE 7 PIP_2-containing GUVs (DOPC/Chol/PIP_2, 80:15:5) in contact with WT and fluorescently labeled ezrin (mixture containing 22 μM of WT ezrin, 100 nM of ezrin-Alexa488, and 100 nM of ezrin-Alexa546). (*A*) Observation of ezrin-Alexa488 (*green channel*), (*B*) of ezrin-Alexa546 (*red channel*), and (*C*) merge of the green and red channels. (*D*) The intensity profile along the GUV circumference is given for both channels (the first point of the lower profile has been set arbitrary at 1 and the upper curve has been shifted for a better visualization). The arrow indicates a cluster visible in both channels. Scale bar: 10 μm.

dye. Thus, ezrin-Alexa488 and ezrin-Alexa546 interacted in a similar way with PIP_2-containing GUVs (Fig. 7 and Table 2). The heterogeneity of the GUVs membranes in the presence of ezrin (as quantified by the signal of FL-PIP_2) was also higher than for GUVs in the absence of ezrin (Fig. 4). We also verified that, for a given GUV, σ/I_{MEAN} did not vary over the observation period (~5 min).

When FL-PIP_2 was used in combination with Ezrin-Alexa546, we observed that FL-PIP_2 and Ezrin-Alexa546 colocalized at the membrane of GUVs and that the distribution of both ezrin-Alexa546 and of FL-PIP_2 appeared non uniform with local increase in concentrations in few clustered regions (Figs. 8 and 4, *last two columns*). Indeed, we measured $\sigma/I_{MEAN} = (31.6 \pm 16.6)$ %, for FL-PIP_2-labeling and $\sigma/I_{MEAN} = (30.5 \pm 14.7)$ %, for ezrin-Alexa546-labeling.

DISCUSSION

Proof for the incorporation of PIP_2 in GUVs

Membranes composed of a very limited number of constituents, like DOPC, cholesterol, and PIP_2 membranes are often used as biomimetic systems to investigate the properties of PIP_2 in the membrane (46) or the interactions of proteins with the membrane (29). Fluorescent labeling by incorporation of fluorescent PIP_2 at 0.1% and/or antibodies that label only a very small fraction of the molecules (between 1:1000 to 1:10,000) is convenient for microscopy observations but does not allow any quantitative determination of the degree of incorporation of PIP_2 molecules in the lipidic membrane of GUVs, whereas ζ-potential measurements could. However, the quantitative incorporation of PIP_2 by ζ-potential measurements has only been proven for multilamellar vesicles (20) and LUVs (22) thus far. This technique is in fact used widely for physico-chemical and pharmaceutical applications of small unilamellar vesicles and LUVs (47), in particular to investigate their stability or the adsorption of cations (48). To the best of our knowledge, measurements of ζ-potential of GUVs have never been reported in the literature previously. Thanks to our measurements of the ζ-potential of GUVs, we were able to provide evidence for i), the effective and quantitative incorporation of PIP_2 in GUVs; ii), the similar behavior of POPS and PIP_2 in terms of incorporation by electroformation; and iii), a good agreement between GUVs and LUVs prepared by different preparation methods using identical lipid solutions. ζ-Potential measurements appear thus as a new, convenient and rapid tool to check for specific charged lipid insertion in GUVs as well as to evaluate their stability in time. Based on these measurements, we found that i), the ζ-potential of the GUVs made from a lipid mixture containing increasing amount of PIP_2 decreases continuously up to a saturation for 8% PIP_2; and ii), GUVs made from a lipid mixture containing DOPC, cholesterol, and PIP_2 (DOPC/chol/PIP_2 80:15:5) are stable for a least 1 day.

Role of divalent ions

Investigating the stability of PIP_2-containing GUVs is particularly important for future applications where actin or other proteins have to be involved. In fact, PIP_2 is known to interact with many actin-binding proteins such as ERM proteins,

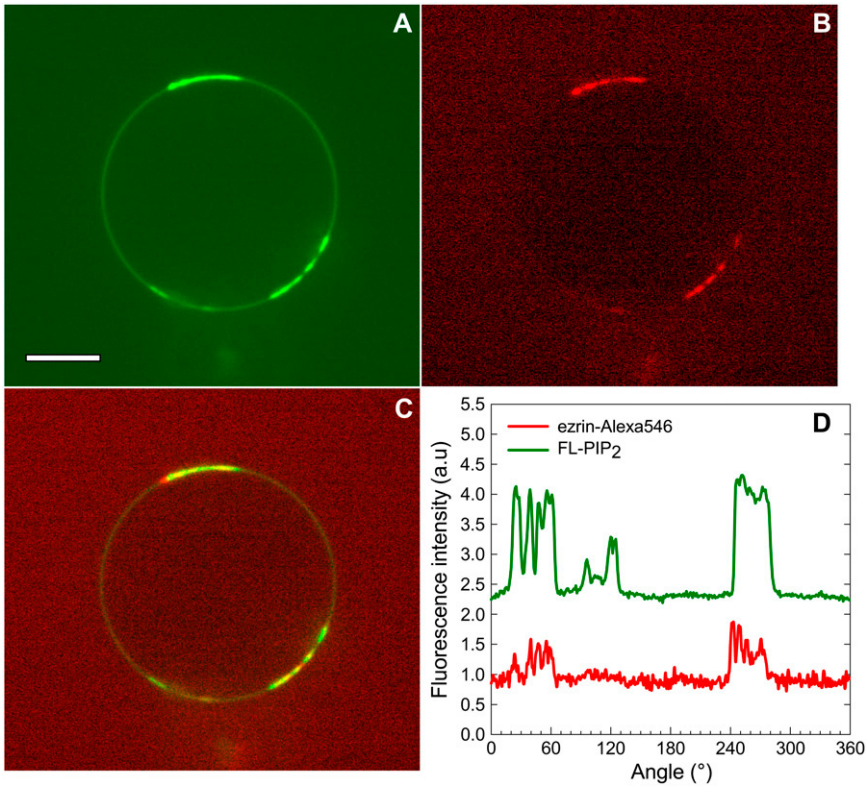

FIGURE 8 Contact between PIP_2-containing GUVs labeled with FL-PIP_2 and ezrin-Alexa546. (*A*) Observation of a GUV containing 0.1% FL-PIP_2 (DOPC/Chol/PIP_2/FL-PIP_2, 80:15:4.9:0.1). (*B*) Same vesicle as in (*A*) observed in the red channel for visualization of ezrin-Alexa546. (*C*) Merge of the two images. (*D*) Intensity profiles for each channel along the circumference of the GUV (the upper curve has been shifted for better visualization). Scale bar: 10 μm.

vinculin, talin, profilin, WASP, and N-WASP (4) and biomimetic systems appear as elegant tools to investigate specific interactions of PIP_2 and actin binding proteins (13,45). Thus, it is important to fully characterize the behavior of PIP_2-GUVs in buffers such as F-actin buffer, which often contains 2 mM $MgCl_2$. In addition, several other proteins like annexins bind to PIP_2 in a Ca^{2+}- dependent manner (14). Moreover, it is known that divalent ions have an affinity for the phosphate groups of PIP_2. Using multilamellar vesicles, McLaughlin et al. (20) estimated the intrinsic association constant of calcium with phosphate groups of PIP_2 at $\sim$500 M^{-1} for Ca^{2+} ions and $\sim$100 M^{-1} for Mg^{2+} ions. These authors also showed that calcium concentrations $<$100 μM do not affect significantly the ζ-potential of PC/PIP_2 vesicles. Our results show that Ca^{2+} and Mg^{2+} induce significant PIP_2 clustering when added at $\sim$30 μM for Ca^{2+} and $\sim$300 μM for Mg^{2+}. Thus, one has to keep in mind that clusters of PIP_2 might preexist when studying GUVs/protein interactions in a F-actin buffer. However, the cellular concentrations of calcium are well below those exerting a deleterious effect on GUVs and most of the magnesium added in the F-actin buffer is complexed with adenosine 5′ triphosphate, as in the cell, and should not alter the stability of GUVs.

Insertion of synthetic fluorescent PIP_2 in the membrane

We showed that long-chain (C16) BODIPY-labeled synthetic PIP_2 molecules are needed to get an effective incorporation of these molecules in the membrane of GUVs and that short-chain (C6)-labeled synthetic PIP_2 did not enter the membrane of GUVs. As observed previously with experiments using LUVs, this simply reflects that a long, more hydrophobic acyl chain will incorporate a lipid membrane much more easily and will have more difficulty escaping from it than a short, less hydrophobic one (45,48,49) Interestingly, these previous results on LUVs seem to extend to membranes of GUVs as well as, to some extent, to cellular membranes. Thus, Bagatolli et al. (29) found that short-chains TMR and FL-PIP_2 do not partition well into the membrane of a GUV. Cho et al. (49) also noticed that the short C6 BODIPY-labeled phosphoinositides were not well localized to the surface membrane but were found equally in cytoplasm. Furthermore, our observations of uniform distributions of TMR-PIP_2 and FL-PIP_2 in GUVs membranes (Fig. 3, *A* and *B*) suggest that PIP_2 molecules do not form domains in DOPC/Chol membranes. This is in agreement with the experimental findings of Fernandez et al. (46) with LUVs and Herrig et al. (12) with PIP_2-containing SLBs.

Protein/GUVs interactions

We used ezrin, a ERM protein, as a model protein for visualizing interactions of proteins with PIP_2-containing GUVs. This protein has been used recently to investigate the hole-opening activity of ERM proteins in the membranes of GUVs. In a previous study, Takeda et al. (27) found that high

concentrations of ezrin (15 μM) were able to open holes in the membranes of GUVs made of phosphatidylcholine and of an anionic lipid phosphatidylglycerol at a 1:1 molar ratio, in a low ionic strength medium. Importantly, ezrin-induced hole formation was insensitive to cholesterol added in the membrane but was sensitive to PIP_2 insertion in the membrane. In this latter case, the hole-opening activity was abolished for GUVs containing 10% PIP_2. Thus, although carried out in a different suspending medium for GUVs of different lipid composition, our experiments confirm that ezrin does not induce hole in liposomal membranes containing PIP_2.

Why relatively high concentrations of ezrin are needed to effectively observe an interaction of ezrin with the membrane of GUVs can be understood from the knowledge of the affinity ($\sim$5 μM for ezrin interaction with PIP_2-containing LUVs (22)) and from the known concentration of lipid in solution. In our experimental conditions, using 15 μM ezrin, 80% of the PIP_2 molecules are expected to be bound (Fig. S1 in Data S1), whereas $<$2.7% of ezrin will be bound. This would explain the profiles given in Fig. 6 *D*, which shows that for GUVs labeled with fluorescent ezrin, the local concentration of ezrin at the membrane is at most about twice the bulk concentration of ezrin.

In addition, our observations suggest that ezrin might be able to reorganize the PIP_2 molecules incorporated in the membrane of GUVs upon interaction. Ezrin appears clustered in some places (Figs. 4 and 6–8). Such clustering was already observed by AFM for ezrin interacting with a SLB containing 3% of PIP_2 and was attributed to protein/protein interactions at the membrane surface (12). Indeed, we found that GUVs observed via PIP_2 antibodies, PIP_2 appear clustered, this clustering being enhanced as the size of the detection complex was increased (Figs. 3, *C* and *D*, and 4). A noticeable difference appears when FL-PIP_2 was observed on the same GUVs (the tertiary antibodies being observed in the red channel): a more homogeneous distribution is visible in the green channel, where the FL-PIP_2 is detected (compare *column 3* and *4* in Fig. 4 *A*). This suggests that the clustering effect observed using antibodies is essentially artifactual and results from the building of large complexes.

CONCLUSIONS

ζ-Potential measurements allow one to follow unlabeled PIP_2 insertion in the membrane of GUVs fabricated by the electroformation technique. Long-chain (C16) fluorescent PIP_2 analogs (TMR-PIP_2 and FL-PIP_2) were used as tracers (0.1%) for visualizing the membrane by confocal microscopy. The homogeneity of the membrane of PIP_2-containing GUVs was quantified using the SD of the fluorescence intensity along the GUV contour and was found to depend of the method of observation: antibodies against PIP_2 appear clustered, the clustering depending on the size of the antibodies, whereas TMR- and FL-PIP_2 appear homogenously distributed in the membrane. The PIP_2-containing GUVs were used for subsequent ezrin/GUVs interaction studies using either fluorescently-labeled GUVs, fluorescently-labeled ezrin, or both. Ezrin was found to interact with the GUVs leading to a reorganization of PIP_2 on interaction. Ezrin bound similarly to GUVs containing only unlabeled PIP_2 or unlabeled PIP_2 with 0.1% FL-PIP_2. Besides a number of transmembrane ligands, ezrin is also an actin binding protein, which justifies its role as a membrane-cytoskeleton linker (50). We believe the characterization of a biomimetic system presented in this study is obviously the first step for understanding the mechanisms of the morphogenic properties of ezrin. More widely, these biomimetic vesicles can also be used for investigation of phosphoinositide containing GUVs with several other types of proteins.

SUPPLEMENTARY MATERIAL

To view all of the supplemental files associated with this article, visit www.biophysj.org.

We are grateful to Michel Terray and Sandrine Vieules from Malvern Instruments for providing the Zeta NanoZS apparatus. We thank Andrea Parmeggiani (Université de Montpellier 2) for fruitful discussions as well as Pierre-Emmanuel Milhiet and Christian Legrimellec (Centre de Biochimie Structurale, Montpellier) for their technical advices. C.P. is a Junior Member of the Institut Universitaire de France whose support is gratefully acknowledged.

This work was supported in part by the European Network of Excellence NoE ''SoftComp'' (NMP3-CT-2004-502235).

REFERENCES

1. Payrastre, B., K. Missy, S. Giuriato, S. Bodin, M. Plantavid, and M. Gratacap. 2001. Phosphoinositides: key players in cell signaling, in time and space. *Cell. Signal.* 13:377–387.
2. Yin, H. L., and P. A. Janmey. 2003. Phosphoinositide regulation of the actin cytoskeleton. *Annu. Rev. Physiol.* 65:761–789.
3. Ling, K., N. J. Schill, M. P. Wagoner, Y. Sun, and R. A. Anderson. 2006. Movin' on up: the role of PtdIns(4,5)P(2) in cell migration. *Trends Cell Biol.* 16:276–284.
4. Niggli, V. 2005. Regulation of protein activities by phosphoinositide phosphates. *Annu. Rev. Cell Dev. Biol.* 21:57–79.
5. Martin, T. F. 2001. PI(4,5)P(2) regulation of surface membrane traffic. *Curr. Opin. Cell Biol.* 13:493–499.
6. Simonsen, A., A. E. Wurmser, S. D. Emr, and H. Stenmark. 2001. The role of phosphoinositides in membrane transport. *Curr. Opin. Cell Biol.* 13:485–492.
7. McLaughlin, S., and D. Murray. 2005. Plasma membrane phosphoinositide organization by protein electrostatics. *Nature.* 438:605–611.
8. Tall, E. G., I. Spector, S. N. Pentyala, I. Bitter, and M. J. Rebecchi. 2000. Dynamics of phosphatidylinositol 4,5-bisphosphate in actin-rich structures. *Curr. Biol.* 10:743–746.
9. Wang, J., A. Gambhir, G. Hangyas-Mihalyne, D. Murray, U. Golebiewska, and S. McLaughlin. 2002. Lateral sequestration of phosphatidylinositol 4,5-bisphosphate by the basic effector domain of myristoylated alanine-rich C kinase substrate is due to nonspecific electrostatic interactions. *J. Biol. Chem.* 277:34401–34412.
10. Hokanson, D. E., and E. M. Ostap. 2006. Myo1c binds tightly and specifically to phosphatidylinositol 4,5-bisphosphate and inositol 1,4,5-trisphosphate. *Proc. Natl. Acad. Sci. USA.* 103:3118–3123.

11. Wagner, M. L., and L. K. Tamm. 2001. Reconstituted syntaxin1a/SNAP25 interacts with negatively charged lipids as measured by lateral diffusion in planar supported bilayers. *Biophys. J.* 81:266–275.
12. Herrig, A., M. Janke, J. Austermann, V. Gerke, A. Janshoff, and C. Steinem. 2006. Cooperative adsorption of ezrin on PIP2-containing membranes. *Biochemistry.* 45:13025–13034.
13. Liu, A. P., and D. A. Fletcher. 2006. Actin polymerization serves as a membrane domain switch in model lipid bilayers. *Biophys. J.* 91:4064–4070.
14. Gokhale, N. A., A. Abraham, M. A. Digman, E. Gratton, and W. Cho. 2005. Phosphoinositide specificity of and mechanism of lipid domain formation by annexin A2-p11 heterotetramer. *J. Biol. Chem.* 280:42831–42840.
15. Buser, C. A., and S. McLaughlin. 1998. Ultracentrifugation technique for measuring the binding of peptides and proteins to sucrose-loaded phospholipid vesicles. *Methods Mol. Biol.* 84:267–281.
16. Rusu, L., A. Gambhir, S. McLaughlin, and J. Radler. 2004. Fluorescence correlation spectroscopy studies of peptide and protein binding to phospholipid vesicles. *Biophys. J.* 87:1044–1053.
17. Richter, R. P., and A. R. Brisson. 2005. Following the formation of supported lipid bilayers on mica: a study combining AFM, QCM-D, and ellipsometry. *Biophys. J.* 88:3422–3433.
18. Baumgart, T., S. T. Hess, and W. W. Webb. 2003. Imaging coexisting fluid domains in biomembrane models coupling curvature and line tension. *Nature.* 425:821–824.
19. Staneva, G., M. Seigneuret, K. Koumanov, G. Trugnan, and M. I. Angelova. 2005. Detergents induce raft-like domains budding and fission from giant unilamellar heterogeneous vesicles: a direct microscopy observation. *Chem. Phys. Lipids.* 136:55–66.
20. Toner, M., G. Vaio, A. McLaughlin, and S. McLaughlin. 1988. Adsorption of cations to phosphatidylinositol 4,5-bisphosphate. *Biochemistry.* 27:7435–7443.
21. Sengupta, P., M. J. Ruano, F. Tebar, U. Golebiewska, I. Zaitseva, C. Enrich, S. McLaughlin, and A. Villalobo. 2007. Membrane-permeable calmodulin inhibitors (e.g., W-7/W-13) bind to membranes, changing the electrostatic surface potential: dual effect of W-13 on epidermal growth factor receptor activation. *J. Biol. Chem.* 282:8474–8486.
22. Blin, G., E. Margeat, C. Royer, C. Roy, and C. Picart. 2008. Quantitative analysis of the interaction of ezrin with large unilamellar vesicles containing phosphatidylinositol(4,5) bisphosphate. *Biophys. J.* 94:1021–1033.
23. Akashi, K., H. Miyata, H. Itoh, and K. Kinosita, Jr. 1996. Preparation of giant liposomes in physiological conditions and their characterization under an optical microscope. *Biophys. J.* 71:3242–3250.
24. Mathivet, L., S. Cribier, and P. F. Devaux. 1996. Shape change and physical properties of giant phospholipid vesicles prepared in the presence of an AC electric field. *Biophys. J.* 70:1112–1121.
25. Rodriguez, N., F. Pincet, and S. Cribier. 2005. Giant vesicles formed by gentle hydration and electroformation: a comparison by fluorescence microscopy. *Colloids Surf. B Biointerfaces.* 42:125–130.
26. Gambhir, A., G. Hangyas-Mihalyne, I. Zaitseva, D. S. Cafiso, J. Wang, D. Murray, S. N. Pentyala, S. O. Smith, and S. McLaughlin. 2004. Electrostatic sequestration of PIP2 on phospholipid membranes by basic/aromatic regions of proteins. *Biophys. J.* 86:2188–2207.
27. Takeda, S., A. Saitoh, M. Furuta, N. Satomi, A. Ishino, G. Nishida, H. Sudo, H. Hotani, and K. Takiguchi. 2006. Opening of holes in liposomal membranes is induced by proteins possessing the FERM domain. *J. Mol. Biol.* 362:403–413.
28. Golebiewska, U., A. Gambhir, G. Hangyas-Mihalyne, I. Zaitseva, J. Radler, and S. McLaughlin. 2006. Membrane-bound basic peptides sequester multivalent (PIP2), but not monovalent (PS), acidic lipids. *Biophys. J.* 91:588–599.
29. Moens, P. D., and L. A. Bagatolli. 2007. Profilin binding to sub-micellar concentrations of phosphatidylinositol(4,5)bisphosphate and phosphatidylinositol(3,4,5)trisphosphate. *Biochim. Biophys. Acta.* 1768:439–449.
30. Sugiura, Y. 1981. Structure of molecular aggregates of 1-(3-*sn*-phosphatidyl)-L-myo-inositol 3,4-bis(phosphate) in water. *Biochim. Biophys. Acta.* 641:148–159.
31. Roy, C., M. Martin, and P. Mangeat. 1997. A dual involvement of the amino-terminal domain of ezrin in F- and G-actin binding. *J. Biol. Chem.* 272:20088–20095.
32. Angelova, M. I., S. Soleau, P. Meleard, J. F. Faucon, and P. Bothorel. 1992. Preparation of giant vesicles by external AC fields. Kinetics and application. *Prog. Colloid Polym. Sci.* 89:127–131.
33. Romer, W., L. Berland, V. Chambon, K. Gaus, B. Windschiegl, D. Tenza, M. R. Aly, V. Fraisier, J. C. Florent, D. Perrais, C. Lamaze, G. Raposo, C. Steinem, P. Sens, P. Bassereau, and L. Johannes. 2007. Shiga toxin induces tubular membrane invaginations for its uptake into cells. *Nature.* 450:670–675.
34. Hunter, R. J. 1981. ζ-Potential in Colloid Science. New York: Academic Press.
35. Henriksen, J., A. C. Rowat, and J. H. Ipsen. 2004. Vesicle fluctuation analysis of the effects of sterols on membrane bending rigidity. *Eur. Biophys. J.* 33:732–741.
36. Kakorin, S., U. Brinkmann, and E. Neumann. 2005. Cholesterol reduces membrane electroporation and electric deformation of small bilayer vesicles. *Biophys. Chem.* 117:155–171.
37. Hatzi, P., S. Mourtas, P. G. Klepetsanis, and S. G. Antimisiaris. 2007. Integrity of liposomes in presence of cyclodextrins: effect of liposome type and lipid composition. *Int. J. Pharm.* 333:167–176.
38. Riske, K. A., and R. Dimova. 2005. Electro-deformation and poration of giant vesicles viewed with high temporal resolution. *Biophys. J.* 88:1143–1155.
39. Dimova, R., K. A. Riske, S. Aranda, N. Bezlyepkina, R. L. Knorr, and R. Lipowsky. 2007. Giant vesicles in electric fields. *Soft Matter.* 3:817–827.
40. McLaughlin, S., J. Wang, A. Gambhir, and D. Murray. 2002. PIP(2) and proteins: interactions, organization, and information flow. *Annu. Rev. Biophys. Biomol. Struct.* 31:151–175.
41. Solon, J., O. Gareil, P. Bassereau, and Y. Gaudin. 2005. Membrane deformations induced by the matrix protein of vesicular stomatitis virus in a minimal system. *J. Gen. Virol.* 86:3357–3363.
42. Sandre, O. 2000. PhD thesis, Pores transitoires, adhésion et fusion de vésicules géantes. Paris: University Paris 6. 195 p.
43. Papadopulos, A., S. Vehring, I. Lopez-Montero, L. Kutschenko, M. Stockl, P. F. Devaux, M. Kozlov, T. Pomorski, and A. Herrmann. 2007. Flippase activity detected with unlabeled lipids by shape changes of giant unilamellar vesicles. *J. Biol. Chem.* 282:15559–15568.
44. Cooper, J. A., S. B. Walker, and T. D. Pollard. 1983. Pyrene actin: documentation of the validity of a sensitive assay for actin polymerization. *J. Muscle Res. Cell Motil.* 4:253–262.
45. Heuvingh, J., M. Franco, P. Chavrier, and C. Sykes. 2007. ARF1-mediated actin polymerization produces movement of artificial vesicles. *Proc. Natl. Acad. Sci. USA.* 104:16928–16933.
46. Fernandes, F., L. M. Loura, A. Fedorov, and M. Prieto. 2006. Absence of clustering of phosphatidylinositol-(4,5)-bisphosphate in fluid phosphatidylcholine. *J. Lipid Res.* 47:1521–1525.
47. Takeuchi, H., H. Yamamoto, and Y. Kawashima. 2001. Mucoadhesive nanoparticulate systems for peptide drug delivery. *Adv. Drug Deliv. Rev.* 47:39–54.
48. Garbuzenko, O., S. Zalipsky, M. Qazen, and Y. Barenholz. 2005. Electrostatics of PEGylated micelles and liposomes containing charged and neutral lipopolymers. *Langmuir.* 21:2560–2568.
49. Cho, H., Y. A. Kim, J. Y. Yoon, D. Lee, J. H. Kim, S. H. Lee, and W. K. Ho. 2005. Low mobility of phosphatidylinositol (4,5) bisphosphate underlies receptor specificity of Gq-mediated ion channel regulation in atrial myocytes. *Proc. Natl. Acad. Sci. USA.* 102:15241–15246.
50. Bretscher, A., D. Reczek, and M. Berryman. 1997. Ezrin: a protein requiring conformational activation to link microfilaments to the plasma membrane in the assembly of cell surface structures. *J. Cell Sci.* 110:3011–3018.
51. Tong, J., L. Nguyen, A. Vidal, S. A. Simon, J. H. Skene, and T. J. McIntosh. 2007. Role of GAP-43 in sequestering phosphatidylinositol 4,5-bisphosphate (PIP2) to raft bilayers. *Biophys. J.*